

Consistency and reproducibility in atomic layer deposition

Henrik H. Sønsteby, Angel Yanguas-Gil, and Jeffrey W. Elam

Citation: *Journal of Vacuum Science & Technology A* **38**, 020804 (2020); doi: 10.1116/1.5140603

View online: <https://doi.org/10.1116/1.5140603>

View Table of Contents: <https://avs.scitation.org/toc/jva/38/2>

Published by the [American Vacuum Society](#)

ARTICLES YOU MAY BE INTERESTED IN

[Understanding chemical and physical mechanisms in atomic layer deposition](#)

The Journal of Chemical Physics **152**, 040902 (2020); <https://doi.org/10.1063/1.5133390>

[Conformality in atomic layer deposition: Current status overview of analysis and modelling](#)

Applied Physics Reviews **6**, 021302 (2019); <https://doi.org/10.1063/1.5060967>

[Atomic layer deposition of functional multicomponent oxides](#)

APL Materials **7**, 110901 (2019); <https://doi.org/10.1063/1.5113656>

[Photoassisted atomic layer deposition of oxides employing alkoxides as single-source precursors](#)

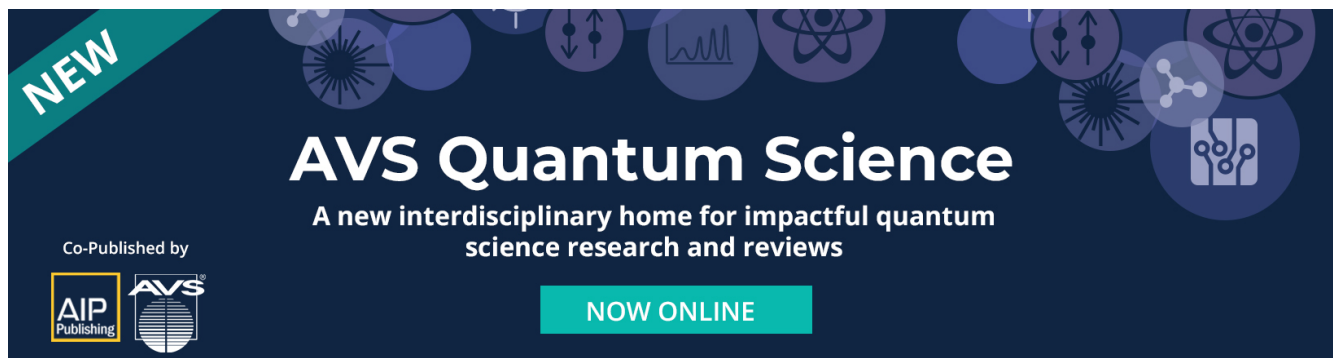
Journal of Vacuum Science & Technology A **37**, 060911 (2019); <https://doi.org/10.1116/1.5124100>

[The chemical physics of sequential infiltration synthesis—A thermodynamic and kinetic perspective](#)

The Journal of Chemical Physics **151**, 190901 (2019); <https://doi.org/10.1063/1.5128108>

[Status and prospects of plasma-assisted atomic layer deposition](#)

Journal of Vacuum Science & Technology A **37**, 030902 (2019); <https://doi.org/10.1116/1.5088582>



NEW

AVS Quantum Science

A new interdisciplinary home for impactful quantum science research and reviews

Co-Published by



NOW ONLINE

The banner features a dark blue background with a teal diagonal stripe in the top left corner containing the word 'NEW'. The main title 'AVS Quantum Science' is in large white font. Below it, the subtitle 'A new interdisciplinary home for impactful quantum science research and reviews' is in smaller white font. The logos for 'AIP Publishing' and 'AVS' are shown in the bottom left. A teal button with the text 'NOW ONLINE' is in the bottom right. The background is decorated with various circular icons representing quantum science concepts like atoms, molecules, and data plots.

Consistency and reproducibility in atomic layer deposition

Cite as: J. Vac. Sci. Technol. A **38**, 020804 (2020); doi: [10.1116/1.5140603](https://doi.org/10.1116/1.5140603)

Submitted: 29 November 2019 · Accepted: 21 January 2020 ·

Published Online: 6 February 2020



Henrik H. Sønsteby,^{1,2,a)}  Angel Yanguas-Gil,¹  and Jeffrey W. Elam^{1,3} 

AFFILIATIONS

¹Applied Materials Division, Argonne National Laboratory, Argonne, Illinois 60439

²Department of Chemistry, University of Oslo, Blindern, 0315 Oslo, Norway

³Advanced Materials for Energy-Water Systems (AMEWS) Energy Frontier Research Center (EFRC), Lemont, Illinois 60439

Note: This paper is part of the Special Topic Collection on Reproducibility Challenges and Solutions.

a) Electronic mail: henrik.sonsteby@kjemi.uio.no

ABSTRACT

Atomic layer deposition (ALD) is a thin film synthesis technique that can provide exquisite accuracy and precision in film thickness and composition even on complex, large area substrates. Based on self-limiting surface chemistry, ALD can be insensitive to process conditions and reactor designs, allowing an ALD process developed in one lab to be easily reproduced in other labs. In practice, however, ALD is sometimes difficult to reproduce or replicate, and the results can vary substantially between ALD reactors and between labs. This is exemplified by large deviations in reports on the growth of, e.g., Al_2O_3 , FeO_x , and TiO_2 given the same precursors under similar conditions. Furthermore, the problem of irreproducibility seems to be growing as ALD is adopted by more researchers and integrated into new applications. In this article, the authors highlight some of the major sources of variations and errors and common misconceptions related to ALD. In particular, the authors focus on issues related to precursors, substrates, and deposition tools. The authors illustrate these problems through examples from the literature, and they present results from numerical simulations that describe how nonidealities would manifest in thickness profiles in a typical cross-flow reactor. They also describe how reproducibility in ALD is linked to consistent experimental practice and reporting between labs. The authors' hope is that by educating newcomers to ALD and advocating for consistent reporting of deposition conditions, they can minimize irreproducibility and enable ALD practitioners to realize the full potential afforded by self-limiting surface chemistry.

© 2020 Author(s). All article content, except where otherwise noted, is licensed under a Creative Commons Attribution (CC BY) license (<http://creativecommons.org/licenses/by/4.0/>). <https://doi.org/10.1116/1.5140603>

I. INTRODUCTION

Atomic layer deposition (ALD) is expanding in popularity and scope, with an almost exponential growth in papers published and theses submitted since the beginning of the third millennium.^{1,2} In 2017, more than one in every thousand scientific articles in the Expanded Science Citation Index (SCI-E) utilized or discussed ALD {1862 articles, search terms [TI=(“atomic layer deposition” OR ALD OR “atomic layer epitaxy” OR “molecular layer deposition”) OR TS=(“atomic layer deposition” OR ALD OR “atomic layer epitaxy” OR “molecular layer deposition”)], 2017}. This made ALD one of the most published thin film deposition techniques in 2017, surpassed only by chemical vapor deposition (CVD) and sputtering. Alvaro *et al.*'s characterization of the field and its community in 2018 showed that the technological applications for ALD

have expanded far beyond the successful implementation as gate oxides in transistors to encompass photovoltaics, catalysis, energy storage, and nonvolatile memory, among others.² This has led to a large expansion of the field and a transition from a community comprised mainly of ALD specialists to a much larger group of ALD users that specialize in other fields but employ ALD to achieve their scientific goals. Concurrent with these transitions has been a growth in commercial vendors offering relatively inexpensive ALD tools. The result is a synergistic effect with more and more ALD research being carried out and published every year.

Rapid expansion comes with many advantages; the ALD technique now boasts a diverse library of chemistries (for instance, nearly 800 ALD processes had already been reported by 2013).³ Many ALD materials can be prepared by a range of processes,

allowing the selection of chemistry based on particular temperature requirements, precursor compatibility, or substrates.^{3–5} The swift growth of the field does, however, also pose some significant challenges. One of these challenges is the lack of consistent reporting and the frequent failure to adequately describe operating procedures in sufficient detail to reproduce the process. This has introduced an element of uncertainty to the ALD library where crucial parameters and results can sometimes vary greatly.

An example of this is found in articles dealing with, arguably, the most investigated ALD process: Al₂O₃ from trimethylaluminum (TMA) and water on Si-OH-terminated surfaces. Peer-reviewed reports of the growth per cycle (GPC) range from around 1 to almost 3 Å/cycle (Refs. 6–9) under essentially identical conditions.

Another example with substantial differences in reported growth is the deposition of iron oxides (FeO_x) using bis(cyclopentadienyl) iron [Fe(cp)₂] and O₃ on Si-OH-terminated substrates. This process has been utilized to deposit a range of iron oxides and is also heavily used in the deposition of complex ferrates. GPCs ranging from 0.2 to 1.4 Å/cycle have been reported in the relatively narrow range of 200–300 °C and can clearly not all be correct.^{10–13} It is speculated that parameters involving O₃ play a crucial role in these deviations.

A third example can be found for the deposition of TiO₂ using titanium(IV) isopropoxide (TTIP) and H₂O as precursors. For this process, the inaugural work proposed a GPC of 0.3 Å/cycle between 225 and 325 °C, whereas later reports suggest anything between 0.15 and 1.5 Å/cycle in this temperature interval.^{14–16} The varying GPC, especially at higher temperatures, is believed to be a result of pyrolytic decomposition of adsorbed TTIP molecules (Fig. 1).¹⁷ These deviations are sometimes subtle but may have a profound impact on the functionality of the deposited film.

Of course, some variation in growth is expected from run-to-run and lab-to-lab given the finite level of control over process parameters such as temperature, gas flow, and valve timing as well as measurement uncertainties. However, the growth variations described above for Al₂O₃, FeO_x, and TiO₂ ALD far exceed these expectations. In continuous thin film growth techniques such as physical vapor deposition where film growth is not dictated by surface chemistry, large growth variations are commonly accepted, at least in a research setting. However, given the self-limiting nature of ALD and the level of understanding of ALD surface chemistry, we can and should expect better agreement between ALD results reported from different laboratories. Indeed, the large differences seen in the ALD library cannot be physical and must derive from easily corrected errors in execution or process control. Large deviations in published results are sometimes attributed to “reactor specific” factors in ALD, but as long as the process exhibits self-limiting surface chemistry, it should be possible to compensate for differences in hardware and replicate the process in any ALD reactor.

An important set of questions arises from these considerations: What makes some ALD processes difficult to reproduce, and why has the community accepted that this is an intrinsic feature of the technique? We believe it is in the best interest of the community to identify the common sources of error that can lead to inaccurate and irreproducible claims. With this article, we try to pinpoint some of the most noteworthy causes of misinterpretation that derive from precursors, substrates, and reactors. Our goal is not to chastise or finger-point but rather to provide helpful guidelines for developing and documenting ALD processes, especially to new researchers in the field. We want to confront irreproducibility in ALD by arming the community with the knowledge to diagnose

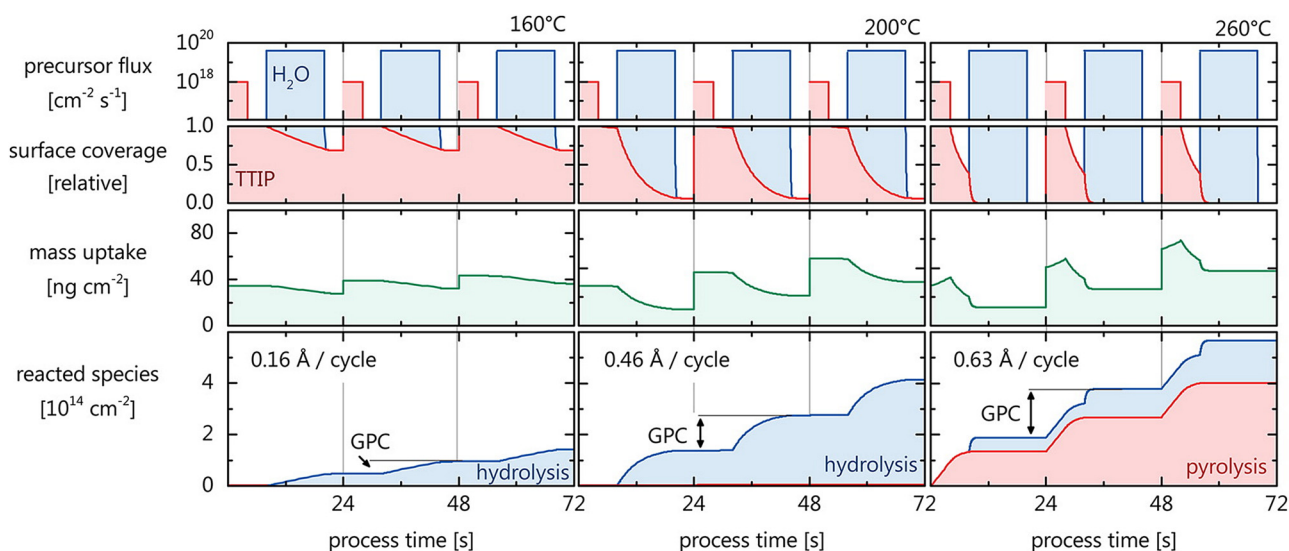


FIG. 1. Number of impinging TTIP and water molecules, relative surface coverage, total mass uptake, and number of reacted TTIP surface species during three ALD cycles at different substrate temperatures. At 160 °C, the hydrolysis rate is too slow to fully hydrolyze the adsorbed TTIP molecules during the water pulse, and at 260 °C, the major fraction of adsorbed TTIP molecules decompose pyrolytically, which is detrimental to the ALD process as the growing film thickness on the substrate will be a function of the precursor flow and, therefore, inhomogeneous and not conformal. Reprinted with permission from Reinke *et al.*, *J. Phys. Chem. C* **120**, 4337. Copyright 2019, American Chemical Society (Ref. 17).

problems and by encouraging experimental scrutiny and transparent reporting.

II. WHEN IS A PROCESS ALD?

ALD is the preferred technique to grow conformal and chemically uniform thin films with angstrom-level accuracy and precision in coating thickness and composition. ALD has been the topic of numerous excellent reviews and we reference only a few of them here.^{18–20} It is not our intention to discuss the many aspects of ALD in detail here, but for the purposes of the present article, it is helpful to single out the defining characteristics of atomic layer deposition. Simply put, when is a process ALD?

In its theoretical form, ALD is a technique as simple as it is brilliant. A substrate is exposed to a gaseous precursor, A, that chemisorbs on accessible sites on its surface and (importantly) does not react with itself. When there are no more available sites, the reaction self-terminates and the substrate surface is considered saturated. At this stage, excess A is purged out of the chamber, and a second precursor, B, is introduced, reacting with the available sites created by A. Upon saturation of B, the reaction again self-terminates resulting in a layer of binary A*B*. These reactions are collectively known as a cycle, and this cycle can be repeated the necessary number of times to obtain the desired film thickness (Fig. 2). Note that more precursor species can be sequentially introduced inside the cycle to obtain ternary, quaternary, etc., layers.^{21–23} The characteristic of ALD growth is the self-limiting nature of all the reaction subcycles inside the cycle. Given a set of conditions (substrate type, substrate preparation, precursor size, precursor reactivity, pressure, temperature, chemical environment, etc.), the concentration of the chemisorbed precursor on the surface at saturation is to be considered an unambiguous value, i.e.,

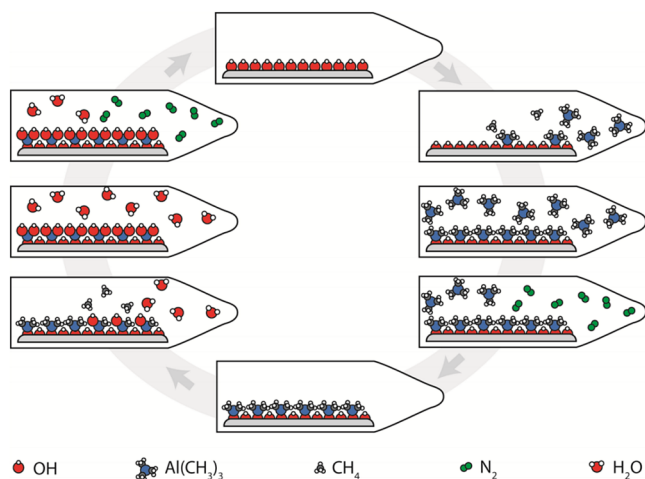


FIG. 2. Cartoon of an ALD cycle, here exemplified by growth of a layer of Al_2O_3 using trimethylaluminum and water as precursors and nitrogen as the purging gas. This cycle is repeated to deposit the desired film thickness. Reproduced with permission from Vee, Master's thesis (University of Oslo, 2012) (Ref. 25).

a number that can be calculated.²⁴ This means that the film thickness deposited by one ALD cycle (i.e., GPC) at a certain stage during deposition on a specified substrate, only determined by the concentration of chemisorbed species, can be considered a thumbprint of an ALD process. It simply cannot be different in two different reactors, as long as the reaction conditions are the same. In other words, this should result in stringent and straightforward reproducibility.

It is important to note that GPC is not necessarily constant throughout a deposition; it is very likely not to be. The number of available sites will vary as the film grows, depending on the initial concentration of the reaction sites, nucleation, evolution of film morphology, etc. Linearity of thickness as a function of the number of cycles after an initial nucleation stage was for long considered an intrinsic feature of ALD, and it is still used toward claiming ALD growth. It is important to note that linear growth can be achieved even in the complete absence of self-limiting, saturating growth, i.e., outside ALD conditions. For instance, one can pulse precursors that decompose on a hot surface to grow a film by CVD. So long as each pulse delivers the same number of precursor molecules, the film thickness will increase linearly with “cycles.” It is also very dangerous to disregard ALD growth on the basis of a lack of linearity. The GPC of many processes are found to change drastically upon the number of cycles, also after initial nucleation. This is exemplified in Fig. 3, showing how the morphology of V_2O_5 films

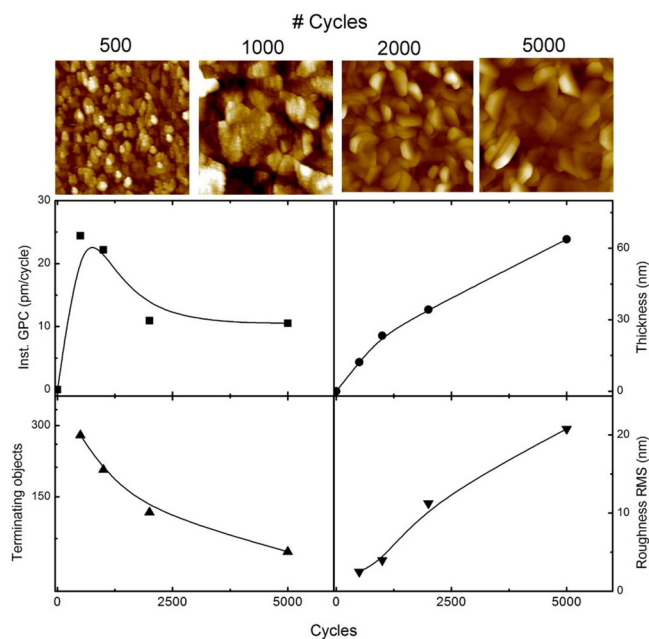


FIG. 3. AFM topography, GPC, thickness, terminating objects, and roughness vs number of deposition cycles for deposition of V_2O_5 using $\text{VO}(\text{thd})_2$ and O_3 . The AFM images are $1.25 \times 1.25 \mu\text{m}^2$ and z-scales are equal. All samples were deposited on Si (111) using 2 s $\text{VO}(\text{thd})_2$ pulse, 1 s purge, 3 s O_3 pulse, and 2 s purge at 186 °C. Reprinted with permission from Østrem *et al.* J. Phys. Chem. C 116, 19444. Copyright 2012, American Chemical Society (Ref. 26).

[prepared using $\text{VO}(\text{thd})_2$ and O_3] changes as a function of thickness, which again strongly affects the GPC during the course of deposition.²⁶ Throughout this evolution, saturating growth is maintained as confirmed by quartz crystal microbalance (QCM) studies. The apparent changes in GPC reflect changes in the substrate surface area. At the atomic scale, on any planar section of the rough surface depicted in Fig. 3, the chemistry proceeds unchanged and the GPC remains the same.

Another common misconception reported frequently in the ALD literature is necessity for an ALD *temperature window*. The erroneous notion is that over a certain temperature range, the GPC of a process *must* remain constant. This typically applies at temperatures sufficiently high to avoid precursor condensation and achieve appreciable reactivity between the precursor and the substrate, but low enough to prevent precursor decomposition and/or desorption of chemisorbed species from the surface. While it is true that all of the effects detailed above (precursor condensation, precursor decomposition, etc.) must be avoided to achieve ALD, the GPC can still change as a function of temperature while maintaining self-limiting growth. This is possible due to temperature-dependent changes in the concentration of reactive sites on the substrate surface and changes in the reaction pathway of the precursor itself. An example of this was recently observed for ALD of SnS from bis(N,N' -diisopropylformamidinato)tin(II) and H_2S .²⁷ Figure 4 shows how the GPC of this process decreases linearly with increasing temperature, with saturating growth observed over the full temperature range. The decrease in GPC is mainly explained by a decrease in the areal density of thiol groups with increasing

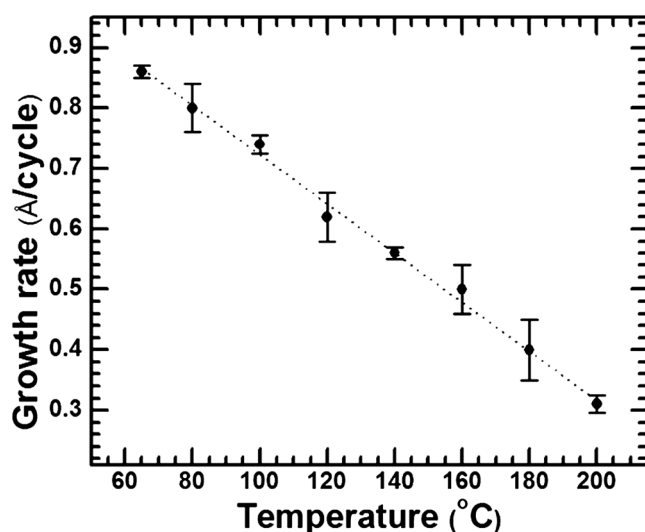


FIG. 4. Variation in SnS ALD growth per cycle with temperature using bis(N,N' -diisopropylformamidinato)tin(II) and H_2S . The error bars represent the range of thickness values measured at three or more locations from one sample or from two samples deposited using the same condition but on different days. Reprinted with permission from Kim *et al.*, ACS Appl. Mater. Interfaces **11**, 45892 (2019). Copyright 2019, American Chemical Society (Ref. 27).

temperature, effectively reducing the number of available chemisorption sites for the tin precursor in the next half cycle.

Another example, with a completely different mechanism, can again be found for growth of V_2O_5 films [$\text{VO}(\text{thd})_2 + \text{O}_3$], where the GPC is strongly affected by the temperature due to temperature-dependent morphology changes, while still observing saturating and self-limiting growth across the temperature range (Fig. 5).²⁶

It is also important to note that a window of constant GPC can be observed even in the complete absence of self-limiting surface chemistry, i.e., for non-ALD growth. For instance, at a sufficiently high temperature, CVD transitions from reaction-limited to flux-limited at which point the growth rate remains constant as the substrate temperature increases.

The characteristic of ALD growth should instead be found at the core of its chemical principles: *saturation*. As long as within all subcycles in a process there exist a pulse and purge duration where growth is no longer taking place with additional time of exposure or purge, the growth should be considered ALD in nature. An important side note here is that GPC may be altered upon applying extremely long purging durations. This is due to the slow dehydration that is observed on most metal oxide surfaces, which will reduce the amount of available sites for chemisorption.

Showing saturating growth can either be carried out *ex situ* by varying the duration of exposure and purge for the different precursors in use [Fig. 6(a)] or *in situ* by the means of QCM, ellipsometry, or some other technique that can identify termination of growth [Figs. 6(b) and 6(c)]. This is not to say that linearity of

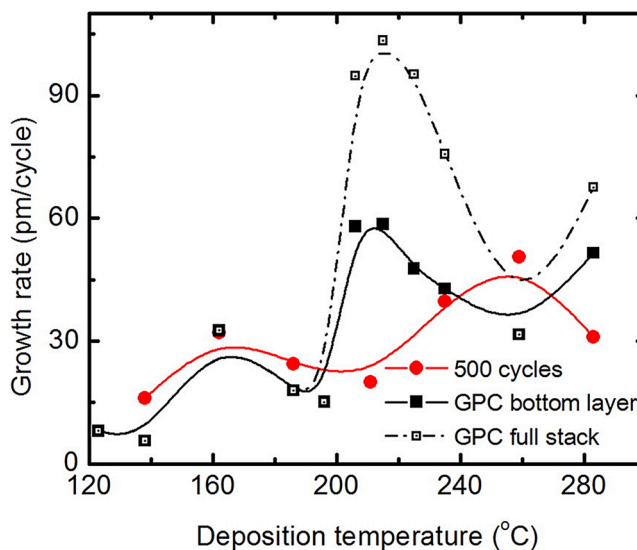


FIG. 5. Evolution in the growth rate of V_2O_5 using $\text{VO}(\text{thd})_2$ and O_3 with deposition temperature for films based on 500 and 2000 cycles. The full symbols symbolize a dense layer, and the open symbols represent the sum of the dense layer and a rough layer (modeled with an effective medium approach). The deposition parameters used are 2 s $\text{VO}(\text{thd})_2$ pulse, 1 s purge, 3 s O_3 pulse, and 2 s purge. Reprinted with permission from Østreg *et al.*, J. Phys. Chem. C **116**, 19 444. Copyright 2012, American Chemical Society (Ref. 26).

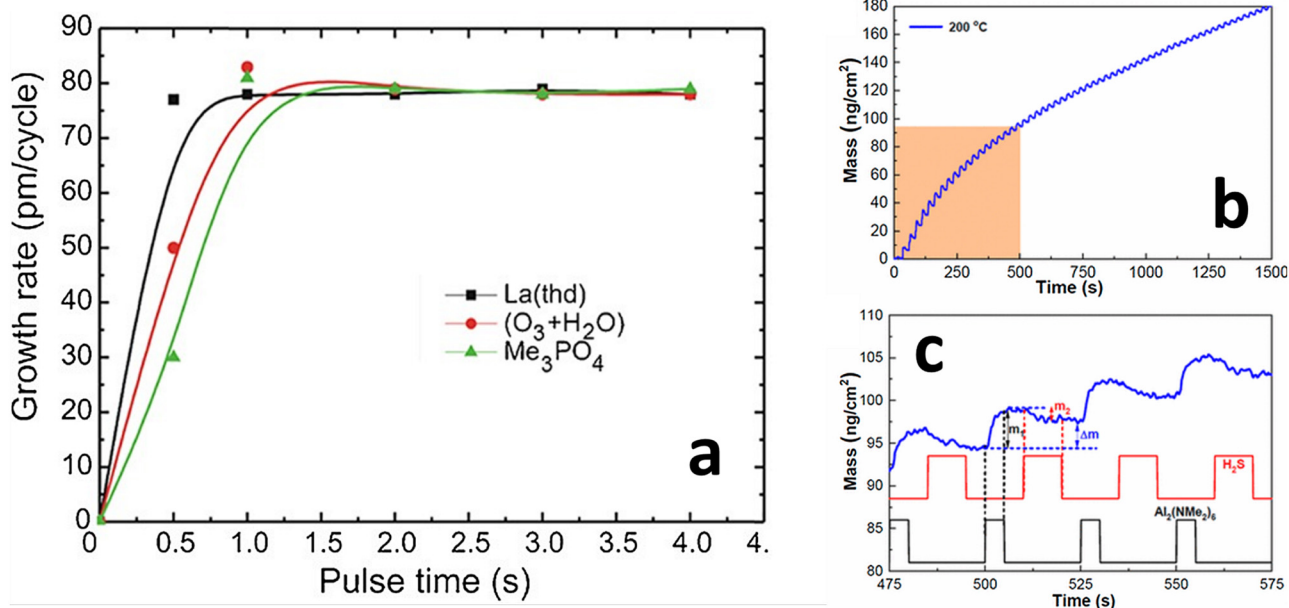


FIG. 6. (a) Growth per cycle for ALD of LaPO₄ using La(thd)₃, (O₃ + H₂O) and Me₃PO₄, as a function of pulse time in seconds. All three precursors show self-limiting, saturating growth, with saturation reached after 0.5, 2, and 2 s, respectively. Reprinted with permission from Sønsteby *et al.*, *Chem. Vapor Depos.* **20**, 269. Copyright 2014, Wiley-VCH Verlag GmbH (Ref. 28). (b) *In situ* QCM measurements of ALD AlSi₃ by Al₂(NMe₂)₆ and H₂S at 200 °C using the timing sequence 5–5–10–5 s. Mass of AlSi₃ film vs time during 60 ALD cycles beginning on ALD Al₂O₃ surface. (c) Enlarged view of four consecutive ALD AlSi₃ cycles in the regime of constant growth per cycle. Lower traces indicate precursor pulsing during the alternating Al₂(NMe₂)₆ (black, lower) and H₂S (red, upper) exposures, and m_1 , m_2 , and Δm are described in the text. Reprinted with permission from Meng *et al.*, *Chem. Mater.* **29**, 9043. Copyright 2017, American Chemical Society (Ref. 29).

growth or ALD temperature windows should not be reported. They are most definitely interesting *features* of a process and are essential to be aware of when utilizing a specific process for application, but they are not necessarily indicators of ALD.

To reiterate, both linear growth (constant GPC with increasing cycles) and a “temperature window” (constant GPC with temperature) are common features in ALD, but they are not defining characteristics. Both of these effects can and do appear in non-ALD growth. In contrast, saturation behavior (constant GPC with increasing exposure) is the one and only defining characteristic of ALD. When is the process ALD? The process is ALD when all of the surface reactions saturate, facilitating self-limiting growth.

III. COMMON SOURCES OF ERROR

With the constraints for ALD growth set, we turn to the matter at hand: What common errors can lead to irreproducible results, and how can we identify them? How do they affect growth? If possible, how can we avoid them?

A. External challenges

Several sources of error in ALD trace back to issues not related to the ALD equipment itself, but to the nature of the chemicals used as precursors or materials used as substrates. These issues often result in lack of growth or to uncontrolled growth that is easy to spot due to composition and/or thickness gradients. Sometimes,

however, the erroneous features are very hard to detect, and we will look at some examples of that in this section.

1. Precursors

Precursors are make-or-break for ALD, and precursor chemistry has been frequently studied and reviewed.^{30–32} Pertaining to the previous discussion, successful precursors must have the ability to chemisorb to and saturate a surface, and the reaction must self-terminate after reaching saturation. In addition, the precursors should not decompose or disrupt the substrate (e.g., cause etching) even on prolonged dosing. Finally, the by-products of the surface reactions must also not disrupt the surface reactions or react with the precursors themselves. With these criteria fulfilled, ALD growth is attainable given saturating exposures and sufficient purging.

High volatility and reactivity are typical traits for ALD precursors. This often coincides with high reactivity toward air, via reaction with either oxygen or water vapor. It is also worth mentioning that even the purest of commercially available inert gases have a notable oxygen and/or water content, which can affect the growth, especially for the ALD of reactive metals, such as Al and Fe, and for extremely long purge durations.

For some precursors, e.g., TMA, reaction with air manifests in violent, spewing flames, which is an easy-to-spot signal that this precursor should be handled under inert conditions. Other precursors, however, exhibit much less violent reactions and are tempting

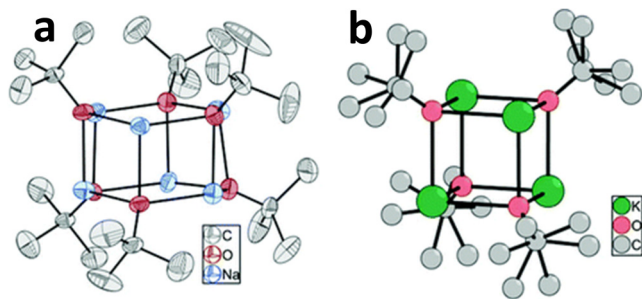
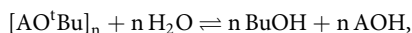


FIG. 7. (a) Molecular structure of NaO^tBu . Hydrogen atoms are omitted for clarity, and thermal ellipsoids showing t -Bu motion are on a 50% level. (b) The previously reported structure of KO^tBu with possible configurations of the disordered methyl groups. Reprinted with permission from Østreg *et al.*, *Dalton Trans.* **43**, 16666 (2014). Copyright 2014, Author(s), licensed under a CCA 3.0 Unported License (Ref. 33).

to handle in air. While brief air exposure is fine for some precursors, there are cases where this can lead to significant reproducibility issues.

One such example is the ALD of alkali metal containing films using t -butoxide precursors. The Na, K, Rb, and Cs t -butoxides are currently the only reported ALD precursors for alkali metal containing films other than lithium.^{33,34} These precursors may look strange at first glance, as the AO^tBu formula indicates a one-ligand metalorganic molecule, which would struggle to create new reaction sites after the initial reaction. However, when dried *in vacuo* after precursor synthesis, the molecules form hexamer (LiO^tBu and NaO^tBu) or tetramer (KO^tBu , RbO^tBu , and CsO^tBu) clusters that are likely maintained in the gas phase, giving them appreciable volatility and surface reactivity (Fig. 7).

These clusters are stable over time under nitrogen or argon gas and do not react with oxygen. They are, however, superbases and readily react with water to form butanol and hydroxides,



where $A = \text{Na, K, Rb, or Cs}$. When exposed to water vapor during handling in air, AOH slowly forms and creates a gel-like substance that encapsulates the precursor molecules. The hydroxides have very low vapor pressures and the gel-like substance effectively blocks evaporation of the cluster precursors, leading to very long pulse times needed to achieve saturation. For KO^tBu , the difference in pulse duration needed for saturation using the pristine precursor and somewhat reacted precursor is more than one order of magnitude (Fig. 8). This effect is hard to spot, and thus it is difficult to attribute variable growth to this error, making it a typical precursor reproducibility issue. This underlines the necessity of understanding the reactivity of precursors in use also outside the reaction chamber, but first and foremost to always report how the precursors have been handled when research is published.

The ALD of TiN by tetrakis(dimethylamino)titanium (TDMAT) and ammonia (or ammonia plasma) is another process that has caused significant reproducibility challenges. On first glance, this

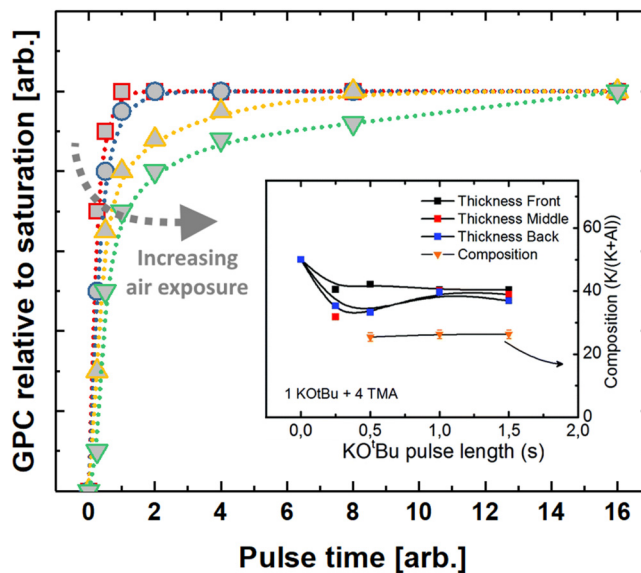


FIG. 8. Theoretical example of how the pulse time needed to reach saturation increases as a function of handling time in air for alkali metal $tert$ -butoxides. Prolonged air handling time drastically increases pulse time needed for saturation. Change in physical appearance of the precursor is almost unnoticeable in the early stages. Inset: Typical saturation curve for potassium $tert$ -butoxide when used together with TMA and water to deposit $\text{K}_x\text{Al}_y\text{O}_z$. Handling time in air was limited to an absolute minimum. Inset reprinted with permission from Østreg *et al.*, *Dalton Trans.* **43**, 16666 (2014). Copyright 2014, Author(s), licensed under a CCA 3.0 Unported License (Ref. 33).

process seems to behave almost ideally, with very high growth rates, a relatively well-defined ALD temperature window, and perfect linearity as a function of the number of deposition cycles (Fig. 9). Moreover, TDMAT has an appreciable vapor pressure at room temperature (~ 0.1 Torr), and this can eliminate the need for additional precursor heating.

The process has been used successfully to deposit very conformal TiN on porous and nonplanar substrates such as ZnO nanoparticles (Fig. 10), suggesting ideal ALD chemistry.

Despite its prevalence and convenience, TDMAT users will often encounter difficulties replicating the results from other labs. Although it is not always stated, TDMAT can decompose at 140°C , and this is frequently below the temperatures used for ALD.³⁷ In fact, a detailed study on TiN ALD using TDMAT and NH_3 found that TDMAT never exhibits true saturation even at 120°C using exposure times of several minutes (Fig. 11).³⁸

This can be attributed to a non-negligible thermal decomposition component that occurs simultaneously with the ALD and becomes noticeable with prolonged dosing. The lack of self-limiting behavior causes the “GPC” to become highly dose-dependent, leading to widely differing reports on the growth rate for ALD using TDMAT and NH_3 (e.g., $0.8\text{--}2 \text{ \AA}/\text{cycle}$ at similar temperatures). The films also exhibit dose-dependent resistivity and porosity due to incomplete reaction of NH_3 with the dimethyl amino surface species leading to variable amounts of dimethyl amino

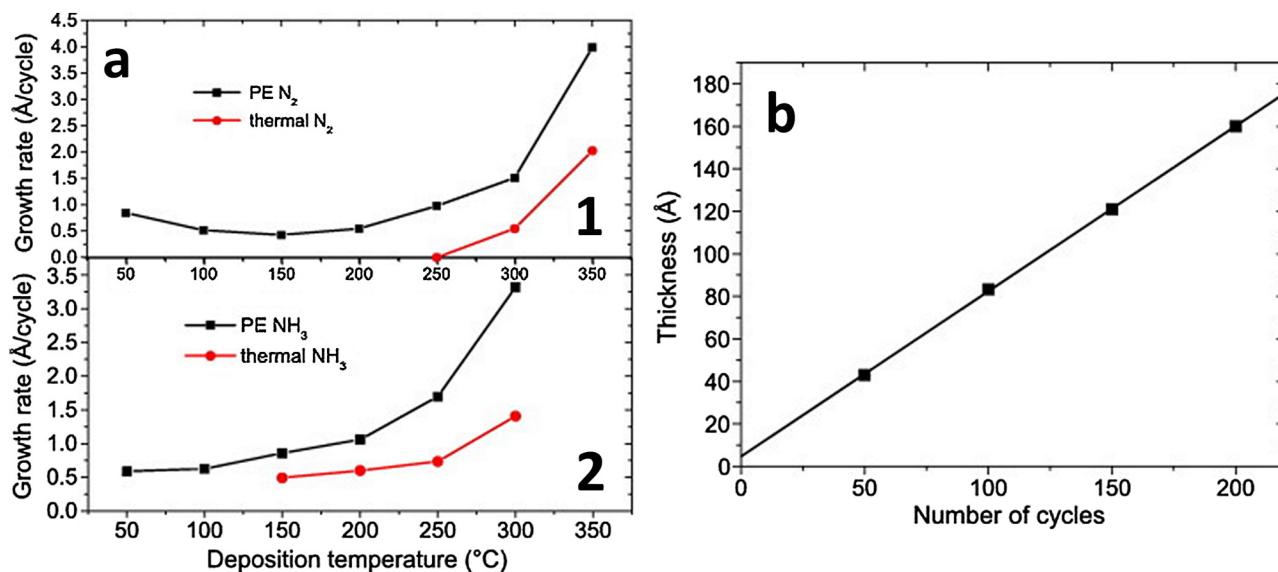


FIG. 9. (a) Growth rate for films (of TiN) deposited using TDMAT and (1) nitrogen and (2) ammonia as reactive gases. Results for thermal and plasma-enhanced processes are shown. (b) Thickness as a function of cycles in the same process. In general, the growth rate for ammonia processes is higher than the corresponding nitrogen ALD. Reprinted with permission from Musschoot *et al.*, *Microelectron. Eng.* **86**, 72. Copyright 2009 Elsevier B.V. (Ref. 35).

residues in the films.³⁸ Although many authors report simply the dose time, the actual precursor dose delivered to the substrate is dictated by many factors including the bubbler temperature (i.e., the precursor vapor pressure), reactor geometry and surface area, bubbler volume, delivery line temperature, and even the thermal history of the precursor since prolonged heating can lead to sintering and surface area reduction for solid phase precursors. These

effects can complicate the task of replicating a published ALD process in a different reactor. This emphasizes the need to carry out saturation studies at the intended deposition temperatures and the importance of reporting these values. TDMAT is certainly not

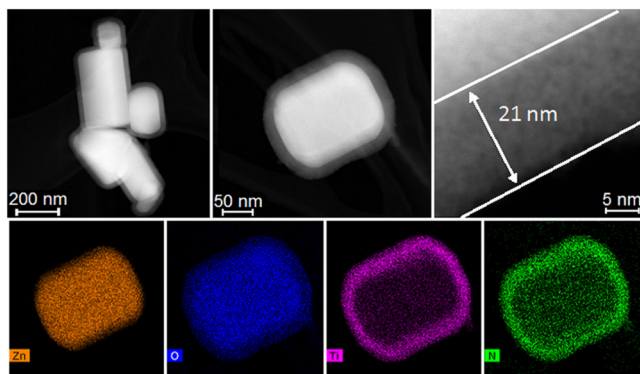


FIG. 10. TEM images of ZnO crystals of different size and shape coated with 300 cycles (21 nm) of amorphous TiN with the Plasma-Enhanced Atomic Layer Deposition (PE-ALD) process (using TDMAT as the titanium source) and energy dispersive x-ray mapping of zinc, oxygen, titanium, and nitrogen of the particle shown in the middle TEM image performed with High-Angle Annular Dark Field Scanning Transmission Electron Microscopy (HAADF-STEM). Reprinted with permission from Longrie *et al.*, *ACS. Appl. Mater. Interfaces* **6**, 7316. Copyright 2014. American Chemical Society (Ref. 36).

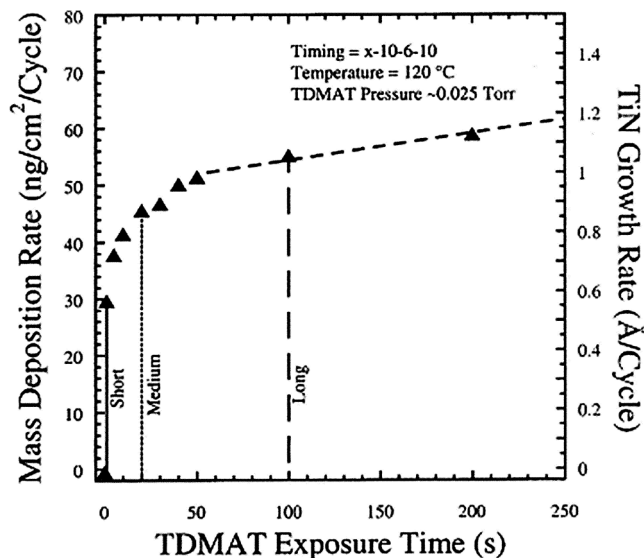


FIG. 11. Mass deposition rate vs TDMAT exposure time at 120 °C on an initial TiN surface terminated with NH_x^{*} species, for deposition of TiN using TDMAT and NH₃ as precursors. Reprinted with permission from Elam *et al.*, *Thin Solid Films* **436**, 145. Copyright 2003, Elsevier B.V. (Ref. 38).

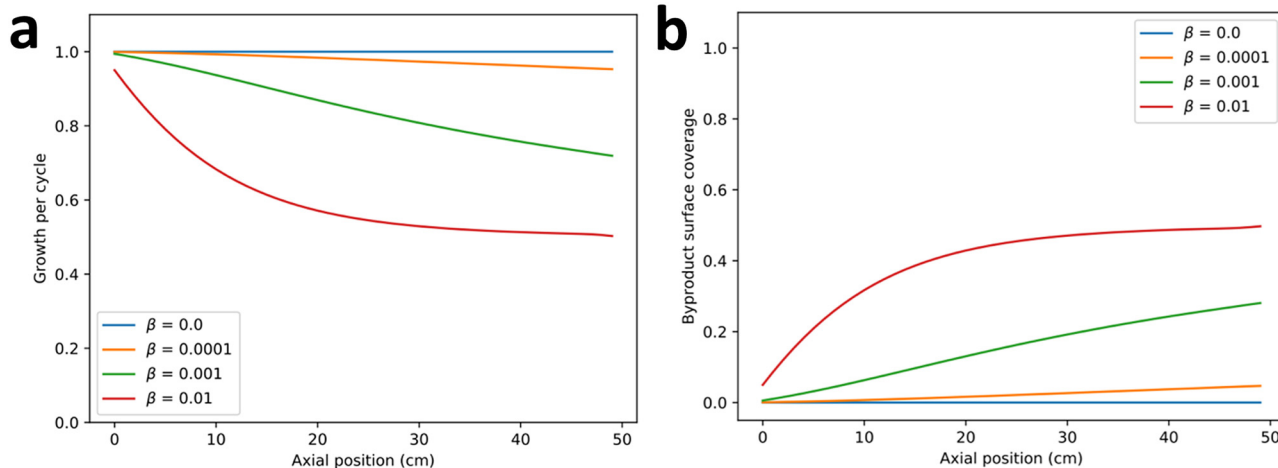


FIG. 12. Impact of ligand competition on saturated growth profiles in a cross-flow ALD reactor: (a) normalized growth per cycle; (b) fractional coverage of ligands on the surface after the precursor dose. Results are shown as a function of the sticking probability of ligands. The model assumes that the coreactant is capable of fully removing the ligands from the surface.

the only precursor that has caused issues with reproducibility. Another well-known example is the ALD of TiO_2 and other Ti-containing films using titanium isopropoxide.

Numerical simulations are an effective means for visualizing the effects of nonideal surface kinetics. Here, we adapt a 1D transport model for a horizontal reactor and introduce theoretical nonidealities. Details of the model, including the agreement with experimental growth profiles, are shown elsewhere.³⁹ One interesting example in this respect is the effect of competitive adsorption of precursor ligands, which are known to lead to self-limited behavior yet inhomogeneous growth profiles in the reactors.^{14,39} We can incorporate this effect by extending a 1D transport model to consider a ligand species that can compete with the precursor for adsorption and later be displaced by the coreactant. Using such models, it is possible to quantify the impact that the sticking probability of the ligand has on the homogeneity of the resulting growth profile. One such example is shown in Fig. 12, with the resulting growth profiles [Fig. 12(a)], as well as the fraction of surface sites blocked by readsorbed ligands [Fig. 12(b)] after a precursor dose, for an otherwise ideal ALD characterized by irreversible first order Langmuir kinetics. These gradients are obtained even under self-limited conditions. From an experimental perspective, alkoxide and beta-diketonate ligands have been shown to partially inhibit growth of various metal oxides.⁴⁰

The final precursor challenge that we will discuss is perhaps the most elusive and difficult to handle because it may only appear after the ALD film achieves a certain thickness. Some ALD materials, especially transition metal oxides, such as copper-, nickel-, and cobalt oxide, can catalytically decompose metalorganic compounds. This can include the very precursor used to deposit the transition metal such as the commonly used β -diketonates of copper, nickel, and cobalt. For instance, this effect has been observed in the deposition of LaCuO_{3-x} by ALD.⁴¹ This effect can lead to a drop in the GPC if the compound decomposes upstream of the substrate and

becomes depleted, or to a rise in the GPC if the compound decomposes on the substrate and causes CVD. Initially, the ALD process may exhibit self-limitation indicating ideal chemistry and the GPC can be stable for a large number of cycles and over multiple depositions. However, at some point, the GPC starts to increase significantly until it plateaus at a new value (Fig. 13). This value is typically dose-dependent since larger precursor exposures will produce a greater amount of catalyzed decomposition. At this point, the process will not pass a saturation test. Furthermore, the concentration of impurities such as carbon in the film will increase

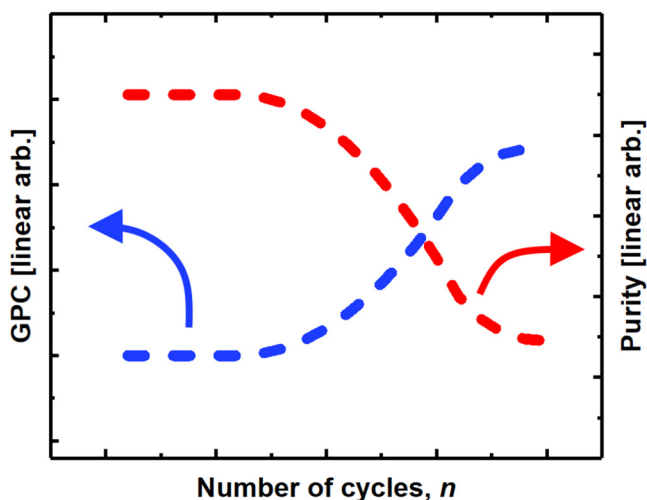


FIG. 13. Theoretical dependence on the growth per cycle (GPC, blue, left axis) and purity (red, right axis) as a function of the number of cycles deposited using a precursor for which the deposited film catalytically decomposes the precursor.

significantly. The opposite behavior may be seen if the precursor decomposes on surfaces between the precursor reservoir and the substrate. The GPC measured on the substrate may be steady for a period of time, but upon the onset of surface catalyzed decomposition, the precursor can be consumed upstream of the substrate leading to a decrease in the GPC. Transition metal oxide films can also catalyze ozone decomposition and cause the GPC to decrease if ozone is used as the oxygen source for the metal oxide ALD.⁴² These effects can be particularly troublesome during the ALD of ternary metal oxide compounds since the catalytic decomposition of ozone or metalorganics may only occur over a limited range of compositions. Ozone recombination or peroxide decomposition may cause gradients in the growth per cycle,⁴² and depending on the reactor geometry, it is possible to quantify the impact that recombination probability would have on the resulting growth profiles.³⁹

These effects are intrinsic to the surface chemistry and can violate the self-limitation requirement of ALD. Very often, the catalytic decomposition of ALD precursors manifests as spatial gradients in film thickness and composition, but these will depend strongly on reactor geometry and growth conditions. As a consequence, the catalytic decomposition of ALD precursors is a serious challenge to reproducibility, especially between different labs and different reactors.

There are several strategies for minimizing the effects of ALD precursor catalytic decomposition. First, one can design the reactor to separate the inlet lines for the metal precursor and the oxygen source to minimize the upstream region where both precursors flow. This will limit the surfaces available for catalytic decomposition. Next, one can select a precursor temperature sufficiently high to saturate the ALD surface reactions but below the onset temperature for surface catalyzed decomposition (Fig. 14). In the case of

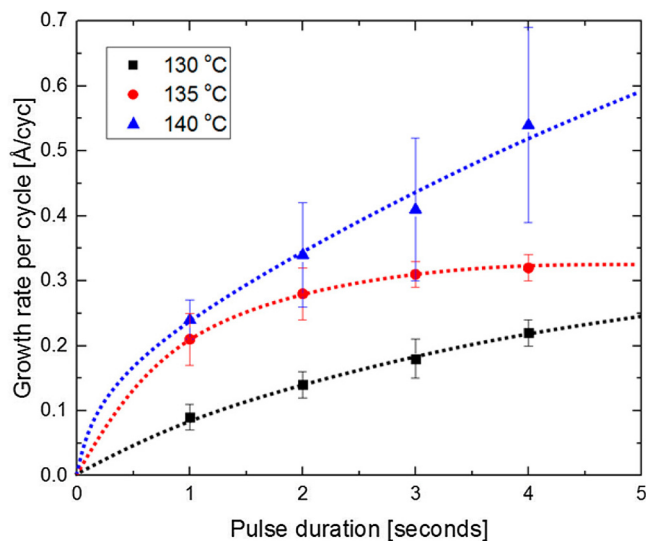


FIG. 14. Growth rate per cycle of CuOx as a function of precursor temperature and pulse duration, using Cu(acac)₂ and O₃ as precursors at a reactor temperature of 250 °C. Reprinted with permission from Sønsteby *et al.*, Chem. Mater. 30, 1095. Copyright 2018, American Chemical Society (Ref. 41).

ozone decomposition, it may be possible to eliminate the ozone and substitute a different oxygen source.⁴³

It is important to note that the effects of surface catalyzed precursor decomposition might manifest only after multiple depositions without exposing the reactor to air in between. In such cases, the effect can be mitigated by passivating the reaction chamber. For instance, one could deposit a layer of inert material such as Al₂O₃ that does not catalyze precursor decomposition between deposition runs of the catalytically active oxides. As mentioned above, this effect can sometimes disappear when depositing a ternary material in which only one of the constituents is catalytically active.⁴¹ This may be thought of as an *in situ* surface passivation that takes place as the process runs.

We finalize our discussion on reproducibility issues caused by precursors by again stressing the importance of careful reporting when publishing ALD processes. The three cases we have highlighted are not an exhaustive list and other challenges exist. These include purity considerations for solid, liquid, and gaseous precursors, which may have significant effects on the reaction mechanism. Imagine, e.g., the large difference in reactivity and saturation time you might get when pulsing 1% O₃ in O₂, compared to 20% O₃ in O₂. While this would only manifest itself in longer pulses needed for lower concentrations of O₃ in many processes, it might completely change the reactivity of the system in others. Also note that ozone behaves very different under different reactor conditions. The half-life of O₃ ranges from days at ambient to seconds at 250 °C. The time (i.e., flow distance) over which O₃ experiences elevated temperatures will strongly affect the true concentration of O₃ in the reactor. The O₃ generator performance can depend on initial O₂ purity, generator model, age, and condition leading to changes in delivered O₃ concentration. Ozone decomposition is often surface catalyzed, so that the composition of the reactor walls (which may change during ALD) can profoundly impact the O₃ lifetime. This underpins the importance of transparency of reporting when carrying out ALD using ozone.

Finally, pretreatment of solid precursors (e.g., by sublimation) is another example that may have pronounced effects on the growth, since this can remove unwanted contaminants in the precursors but also modify the morphology of the solid powder or even the structure of the precursor molecules. These issues can be a source of irreproducibility, but transparent reporting can minimize their harmful effects.

2. Substrates

We often regard ALD as a technique that will coat anything and everything. However, this erroneous notion derives from the fact that when all exposed surfaces become coated in the ALD material, the chemistry becomes identical everywhere. In reality, the ALD reactions depend strongly on the starting surface. As we have already stated, ALD is dictated by the number of accessible surface sites for precursor chemisorption. Different substrate material, chemical termination, crystallographic orientation, and even pretreatment method can modulate the concentration of reactive sites on the surface. Some surfaces, such as graphite, do not facilitate growth at all, or at least exhibit a very long initial nucleation delay. This effect can, when controlled, be utilized to deposit films

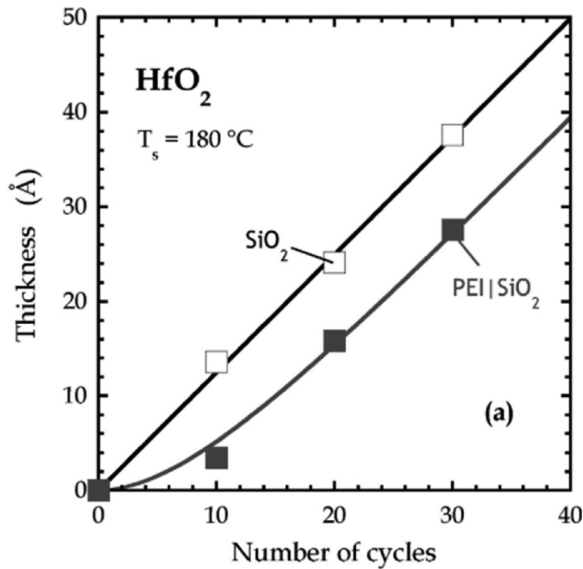


FIG. 15. HfO₂ thin film thickness as a function of ALD cycles on an unmodified SiO₂ substrate (open symbols) and on polyethylene imine coated SiO₂ (PEI/SiO₂, filled). Reprinted with permission from Hughes *et al.*, J. Vac. Sci. Technol. A 30, 01A102. Copyright 2012, American Vacuum Society (Ref. 45).

only on select parts of a substrate, which has given rise to its own subfield: area-selective ALD.⁴⁴ On the other hand, a lack of awareness of these effects may lead to significant replicability issues. For instance, growing a single film and dividing the thickness by the

number of ALD cycles can yield an accurate GPC value only if the ALD film nucleates promptly. Blindly performing the same calculation on a poorly nucleating substrate can yield a much smaller, or even zero, GPC value.

An example of such an effect can be found for hafnium dioxide ALD using tetrakis(ethylmethylenamido) hafnium and H₂O on SiO₂ and polyethylene imine coated SiO₂ (PEI/SiO₂, PEI-layer ~5 Å) substrates (Fig. 15).⁴⁵

A significant nucleation delay can be observed for PEI/SiO₂ substrates leading to ~1 nm difference in film thickness between the two substrates after the same amount of cycles. From 20 cycles onward, the GPC is approximately equal for the two systems. If one were to report an average GPC, let us say after 10 cycles, one would get approximately 1.2 Å/cycle for SiO₂ substrates but only 0.4 Å/cycle for PEI/SiO₂, a difference of 300%. The same study reports that there is no effect on the growth of aluminum oxide using trimethylaluminum and H₂O, while tantalum nitride ALD is even more strongly affected.

Another striking example of the importance of understanding and correctly reporting substrate details can be found for tungsten ALD on a variety of metal oxides with different substrate pretreatment (Fig. 16).⁴⁶

Tungsten ALD on ZnO, Al₂O₃, SiO₂, and TiO₂ surfaces all show different nucleation behaviors, with a difference of growth onset by 20–30 cycles as shown by mass loading measured using *in situ* QCM. On TiO₂, etching of the substrate can be observed before the growth onset. Furthermore, different pretreatments of the substrates play a crucial role in the nucleation delay. *Ex situ* preannealing of the substrates changes the number of cycles needed before the growth onset, which the authors carefully attribute to the concentration of surface hydroxyls as measured by FTIR and

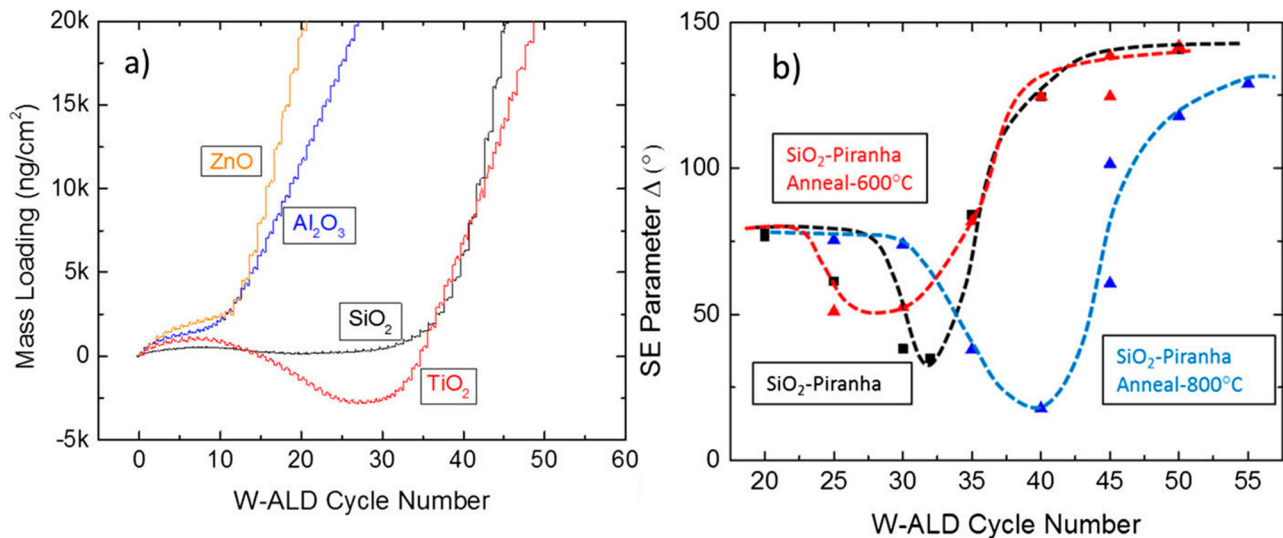


FIG. 16. (a) *In situ* QCM analysis of tungsten metal ALD on ZnO, Al₂O₃, SiO₂, and TiO₂ surfaces. Tungsten deposition is carried out using SiH₄ and WF₆ as precursors. (b) SE delta parameter at 700 nm for SiO₂ samples following W ALD (on substrates with different pretreatments). The W ALD was performed at 220 °C for all samples. Reprinted with permission from Lemaire *et al.*, J. Chem. Phys. 146, 052811. Copyright 2017, AIP Publishing LLC (Ref. 46).

spectroscopic ellipsometry (SE). Vicinal hydroxyl groups (the predominant state after 600 °C anneal) is suggested to support tungsten nucleation, while isolated hydroxyls (predominant state after 800 °C anneal) is suggested to impede the tungsten nucleation.⁴⁶

The last example we would like to highlight in terms of growth variations due to the substrate is the influence of crystallographic orientation on ALD. This is only applicable if the film is growing in an epitaxial manner during the deposition or if the film grows epitaxially on some substrates and amorphous on others. Different crystal planes will have different concentrations of reactive sites, which means that the GPC will be different on the different crystal planes. In general, films where the growth surface is terminated by a high density of chemisorbed precursors tend to grow faster compared to other orientations due to the higher concentration of reactive sites. This also means that the differences in GPC are not found only during the initial nucleation period as discussed above but persist throughout the growth.

Take, for example, the ALD of NiFe₂O₄ (NFO) using nickel acetylacetonate, Fe(cp)₂, and O₃ on two different substrates: MgO (100) and Al₂O₃ (001).⁴⁷ MgO (100) facilitates cube-on-cube growth, with the film growing in the (100)-direction. On the other hand, Al₂O₃ (001) facilitates growth in the (111)-direction, which is also the close-packed planes of the NFO structure. Figure 17 shows the large difference in GPC that is observed for epitaxial growth on these two substrates. The GPC on Al₂O₃ (001) stabilizes at approximately 0.3 Å/cycle after nucleation, while the GPC is only 0.2 Å/cycle on MgO (100). This example demonstrates that for epitaxial films, growth orientation is an important variable that

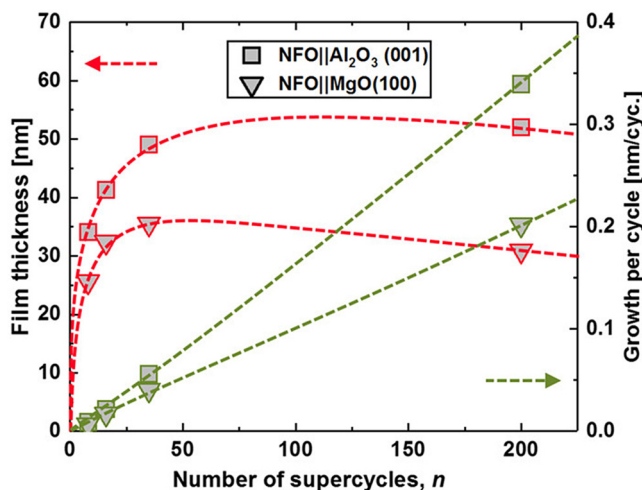


FIG. 17. Film thickness (red, left axis) and growth per supercycle (green, right axis) for NiFe₂O₄ using Ni(acac)₂, Fe(cp)₂, and O₃ as precursors, on Al₂O₃ (001) (squares) and MgO (100) (triangles), as a function of the number of supercycles, *n*. The green (right axis) dashed line is a guide-of-eye line showing the estimated relationship between the pulsed number of supercycles and the film thickness. The red (right axis) line is a guide-of-eye line indicating the relationship between the growth per cycle and the employed number of cycles. Reprinted with permission from Bratvold *et al.*, J. Vac. Sci. Technol. A 37, 021502. Copyright 2019, American Vacuum Society (Ref. 47).

must be carefully considered. It will of course not only alter the growth of the films but also its properties, in this case the direction of the easy axis of magnetization with respect to the film normal.

Nucleation effects during ALD are fairly well documented and understood by the ALD community. However, given the explosive growth of ALD, both in research labs and in the literature, it is likely that newcomers will be unaware of nucleation phenomena leading to confusion and poor reproducibility. To avoid this problem, one has to be careful when reporting the substrate(s) used in a set of experiments. Substrate chemical formula is almost never sufficient, as substrate handling and pretreatment will play a crucial role on nucleation. This pretreatment may be etching by wet chemical treatment or plasma, annealing, or loading with gaseous species on the surface before the onset of deposition. However, it may also be something as simple as how the substrates are stored and handled before placed in the reactor. Furthermore, since nucleation delays will cause confusion if only GPC averages are reported, it is best practice to plot GPC as a function of number of cycles. If that is not possible, then one should at least report how the average GPC has been calculated. Finally, it is also important to consider and report the crystallographic orientation for epitaxial films, as this will almost always affect GPC and properties. Attending to these points will allow for a meaningful comparison between studies and help us to improve reproducibility.

B. Deposition tool

Precursors and substrates are common sources of irreproducibility in ALD that are sometimes difficult to detect. In contrast, problems stemming from the deposition tool are often obvious, appearing as severe thickness gradients and run-to-run variability, but the origin of these problems can be challenging to identify and correct. ALD reactor problems can stem from malfunction or design flaws and include leaks, faulty valves, hot or cold spots, inadequate purging caused by zones of stagnant flow, inadvertent powder formation, or a high internal surface area. The symptoms of these problems depend heavily on the reactor design. We adapted our 1D transport model to visualize the effects of small leaks to air that result in CVD.

In Fig. 18, we show the impact that upstream leaks of the ALD precursor have on the ideal ALD profiles. In particular, we assume that the leak creates a constant background pressure during both doses and purges. We show the impact of such a leak with partial pressure, *p*, normalized to the precursor pressure, *p*₀. Growth is normalized to the ideal growth per cycle, so that values greater than 1 signify the presence of a CVD component. As shown in the figure, leaks of the order of 0.1% are enough to cause a measurable increase in the GPC. This increase in the growth rate is more pronounced in the upstream region of the reactor. However, the spatial distribution depends on the reactivity of the precursor: the model predicts larger yet more confined values when the sticking probability is high [Fig. 16(a)], whereas increases are less pronounced but more homogeneously distributed as the reactivity decreases [Fig. 16(b)].

The inset in Fig. 18(a) shows how an areal thickness gradient may look for a simple reactor with one precursor inlet, one outlet, and flow parallel to the substrate surface. A leak upstream of the

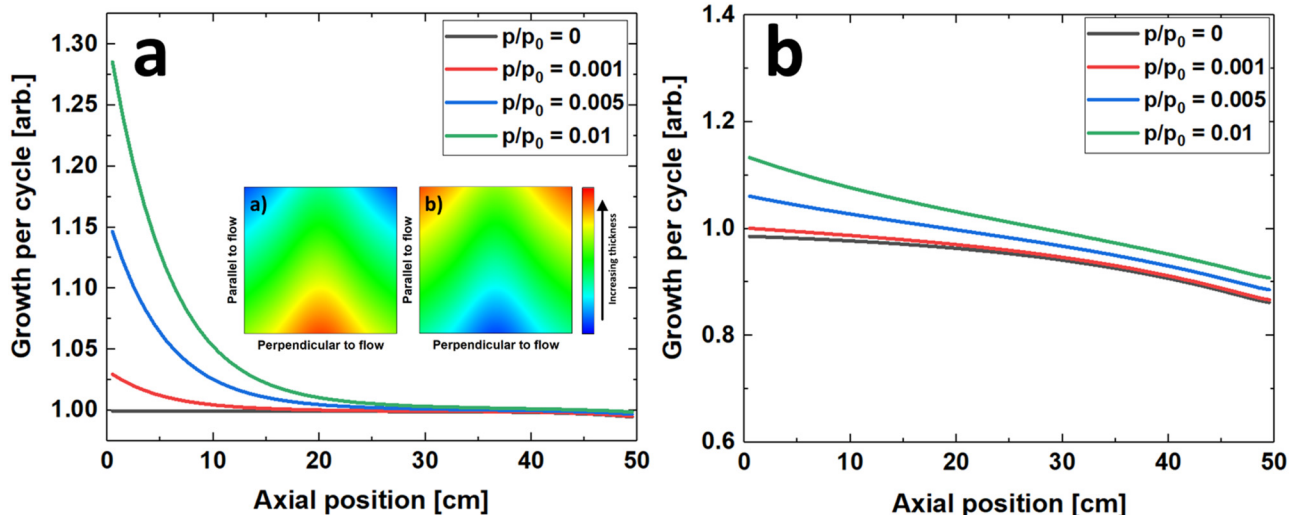


FIG. 18. (a) Impact of upstream leak on growth profiles in a cross-flow reactor. Results are shown for various partial pressures, normalized to the inlet precursor pressure during a dose. Inset: (a) Typical areal thickness gradient for a one inlet, one outlet reactor geometry if there is an upstream leak that increases growth close to the precursor inlet, upstream precursor decomposition, or if pulses of one or more of the precursor pulses are too short. (b) Typical thickness gradient for a one inlet, one outlet reactor geometry if there is a (large) leak downstream or for insufficient purge time.

precursor inlet leads to excessive growth upstream [inset (a) in Fig. 18(a)] while a leak downstream can cause excessive growth near the outlet [inset (b) in Fig. 18(a)]. Thickness gradients can also result from inadequate purge times in a leak-free reactor, but thickness gradients produced by leaks such as the plots in Fig. 18 will persist regardless of the purge time.

Note that very similar effects may result from upstream precursor decomposition or if pulses of one or more of the precursor pulses are too short to reach areal saturation. Usually, deconvoluting leak effects are straightforward by carrying out a saturation study; hence, we will not treat effects like this in detail more here. What we will take a closer look at, however, are less common issues with the reactor or process that may lead to erroneous scientific conclusions, which again hampers reproducibility.

1. Hard-to-spot reactor issues

We introduced this paper by highlighting the very large range of GPC values (<1–3 Å) reported for aluminum oxide ALD using TMA and H₂O by ALD under similar conditions. One issue that undoubtedly contributes to this large variation in reported GPC is the adsorption of H₂O on surfaces upstream of the substrate and subsequent slow release leading to CVD. This effect is commonly referred to as a *virtual leak*, and in ALD, it is often encountered using H₂O at reactor temperatures in the 100–200 °C range. In this range, the H₂O adsorbs to reactor walls but does not so easily purge out. The effect is most prominent when splitting half-cycles into smaller parts by *microdosing*. In Fig. 19(a), we show *in situ* SE measurements performed during Al₂O₃ ALD using TMA and H₂O in a Cambridge Nanotech Fiji F200 ALD system at a temperature of 150 °C exhibiting a GPC value of 1.36 Å/cycle. Increasing the dose

and purge times within “standard” values (e.g., from 0.3 to 1 s) did not affect GPC, indicating that the process is self-limited. In contrast, Fig. 19(b) shows *in situ* SE measurements performed on the same system during successive, 15 ms TMA microdoses separated by 20 s purges, following a 10 s H₂O exposure. Even though no H₂O is dosed between the TMA microdoses, the film continues to grow and achieves a thickness of ~18 Å within the same cycle. This behavior cannot result from a leak to air since the process eventually saturates. A leak to air would never saturate and would give continuous growth while microdosing the TMA. Furthermore, saturation studies performed immediately prior to the experiment in Fig. 18(b) yielded ideal ALD behavior. The effect instead comes from a virtual H₂O leak, likely produced by a cold spot in the reactor where H₂O has condensed and is slowly released during the TMA microdosing. The virtual leak did not affect the measurements in Fig. 18(a) because in this case the TMA and H₂O doses were roughly equivalent so that physisorbed H₂O would react with the subsequent TMA dose, and because the purge times were not sufficient for the physisorbed H₂O to desorb and react on the substrate. In addition, the larger doses of TMA are more likely to react with any physisorbed H₂O in the cold spots. The virtual leaks caused by physisorbed H₂O will magnify over time as powder forms on the cold region since this powder will create a high surface area that adsorbs even more H₂O.

Virtual leaks are a common source of irreproducibility, but these effects can be mitigated by adequately heat tracing the reactor to eliminate cold spots and by designing the reactor to have minimal internal surface area and no stagnant regions that are not purged effectively. Another remedy is to operate at higher deposition temperatures where the H₂O desorption rate is faster or by replacing the H₂O with a noncondensing oxygen source such as O₃

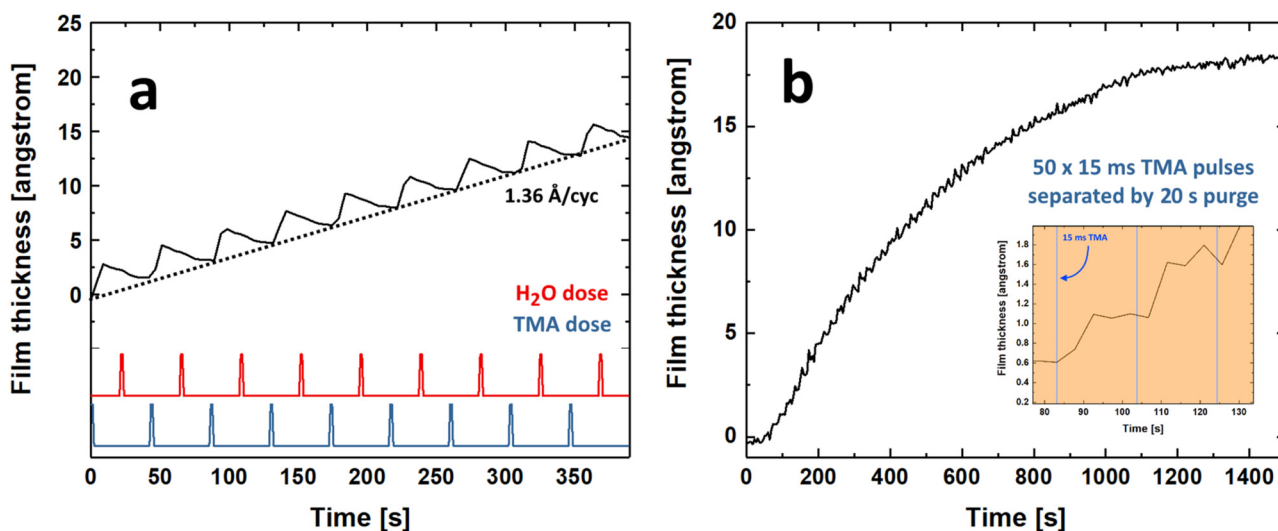


FIG. 19. (a) Typical ALD growth of Al_2O_3 using TMA and H_2O as precursors showing stepwise growth and a GPC of $1.36 \text{ \AA}/\text{cyc}$ as measured by *in situ* spectroscopic ellipsometry. The red (upper) and blue (lower) curves show the timing for H_2O for and TMA doses, respectively. (b) Film thickness as a function of time during $50 \times 15 \text{ ms}$ microdoses of TMA on a surface saturated by $-\text{OH}$ (very long water pulses prior to the TMA microdosing). The inset shows how there is stepwise growth after every microdose.

or oxygen plasma. In situations where H_2O and low deposition temperatures cannot be avoided, one should minimize the H_2O exposures to limit condensation and extend the H_2O purge times to allow adequate time for the H_2O to desorb.

Another reactor issue that may be very hard to spot is *memory effects* during subsequent depositions. This has been observed in variable magnitude for a range of processes, among them the deposition of alkali metals. An example of this is for the deposition of Nb_2O_5 on SiO_x/Si [$\text{Nb}(\text{OEt})_5 + \text{H}_2\text{O} \rightarrow \text{Nb}_2\text{O}_5$, 250°C] immediately following a deposition of K_xNbO_3 (Fig. 20). One can observe a clear trend in the incorporated content of potassium in Nb_2O_5 films depending on the amount of pulsed potassium in the preceding deposition. This does not only affect the composition of Nb_2O_5 but also the growth per cycle. While the effects are relatively small ($<1\%$), they tend to become an accelerated effect for subsequent depositions of K_xNbO_3 . More and more potassium is incorporated in the films, making it very hard to control the composition from deposition to deposition. This potassium contamination and higher growth per cycle likely result from etching of the K_xNbO_3 on the reactor walls by the $\text{Nb}(\text{OEt})_5$ precursor to form volatile potassium compounds that react on the substrate.

One method to avoid this problem is to passivate the reaction chamber with an inert oxide in between runs. Our approach has been to use these Nb_2O_5 depositions as sacrificial passivation runs in between every deposition of KNbO_3 and/or $\text{K}_x\text{Na}_{1-x}\text{NbO}_3$ after which the alkali metal incorporation can be reproduced on a 1% level (Fig. 21). Alternatively, the reactor can be cleaned after each deposition to remove the KNbO_3 and/or $\text{K}_x\text{Na}_{1-x}\text{NbO}_3$ from the reactor walls. This is of course a very tedious approach, and the sacrificial passivation depositions seem to be a less time consuming and convenient way of avoiding these memory effects.

Another example of a passivation effect, or more precisely a *conditioning effect*, has been observed for ALD of cobalt metal thin films from Bis(*N-t*-butyl-*N'*-ethylpropanimidamido)cobalt(II) and hydrogen. When multiple depositions were performed under identical depositions, the uniformity and GPC of the resulting

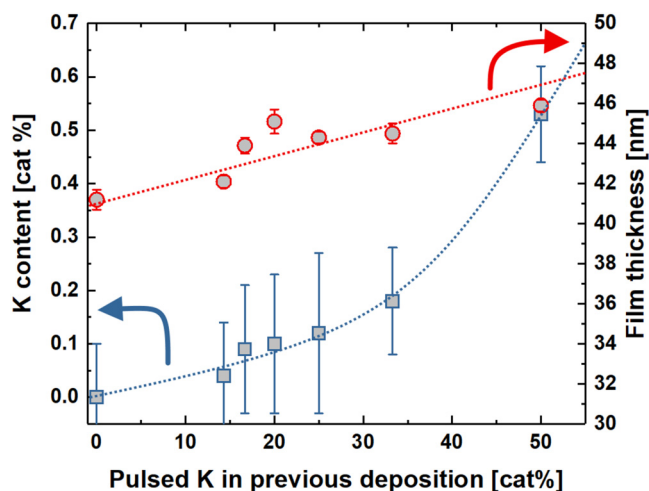


FIG. 20. Potassium content in Nb_2O_5 films deposited at 250°C from niobium ethoxide and water, as a function of the amount of pulsed potassium in the preceding deposition. The blue curve (left axis) shows the potassium content (cat %), while the red curve (right axis) shows the film thickness. Data reproduced with permission from Killi, B.Sc. project thesis (University of Oslo, 2018) (Ref. 48).

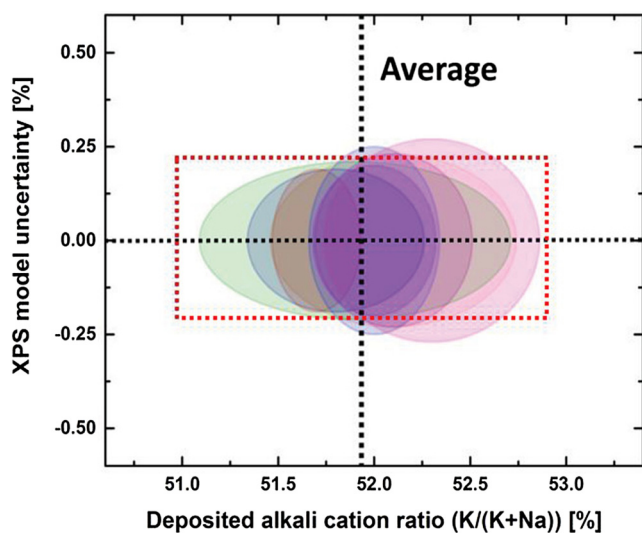


FIG. 21. Eight consecutive depositions (of $K_xNa_{1-x}NbO_3$) using exactly the same parameters (with Nb_2O_5 passivation in between every deposition). Ellipses show the variation in deposited alkali ratio $[K/(K + Na)]$, maximum across all directions in the chamber, x -axis, and the uncertainty in the XPS model, y -direction. The dimensions of the red box (dotted rectangle) illustrate the expected variation in deposited stoichiometry by adding one additional pulse of one of the alkaline elements, x -direction, and the instrumental uncertainty of the XPS system, y -direction. Reprinted with permission from Sonstebj *et al.*, *Glob. Chall.* **2019**, 1800114 (2019). Copyright 2019, Author(s), licensed under a CC BY 4.0 license (Ref. 49).

cobalt metal films were found to depend strongly on the number of preceding depositions (Fig. 22). The researchers found that the reactor had to be conditioned by performing multiple initial cobalt deposition runs before the films became uniform and exhibited a

consistent GPC. If a different ALD process was employed between cobalt depositions, the cobalt conditioning had to be repeated. This effect was particularly strong if the preceding deposition included inorganic-organic hybrid materials. Although the physical reason for this conditioning effect is still unknown, it is clear that documenting the effect is crucial to facilitate reproducibility between labs.

2. Purge

Our final section on reproducibility issues related to the deposition system concerns the purge steps in the ALD cycle. Flushing away the unreacted precursor A before introducing the next pulse of precursor B is essential to maintain a self-limiting growth. If the purge is too short, the A and B precursors will mix in the vapor phase or on the surface causing non-self-limiting CVD. This typically leads to a higher GPC and causes thickness gradients (Fig. 23). On the other hand, excessively long purge times limit productivity and can amplify problems related to impurities in the carrier gas or virtual leaks. For instance, oxygen levels in ALD metal films will scale with the purge time given trace oxygen impurities in the carrier gas. For these reasons, the purge time should be optimized. The optimal purge time is highly reactor specific and is typically smaller (e.g., 1 s) for commercial ALD tools optimized for a particular ALD process and substrate, and larger (e.g., 10 s) for research tools, both commercial and custom built, designed for flexibility to accommodate a variety of substrates and ALD processes. The reactor characteristics that affect purge time are mostly geometric. For instance, the internal (i.e., wetted) surface area dictates the desorption flux of physisorbed precursor, and the cross sectional area controls the flow velocity so that increasing either quantity will increase the precursor residence time in the reactor. Moreover, abrupt geometric transitions (e.g., a narrow precursor inlet pipe connected at right angles to a large, planar reactor wall) will decrease the effectiveness of the carrier gas sweep, necessitating

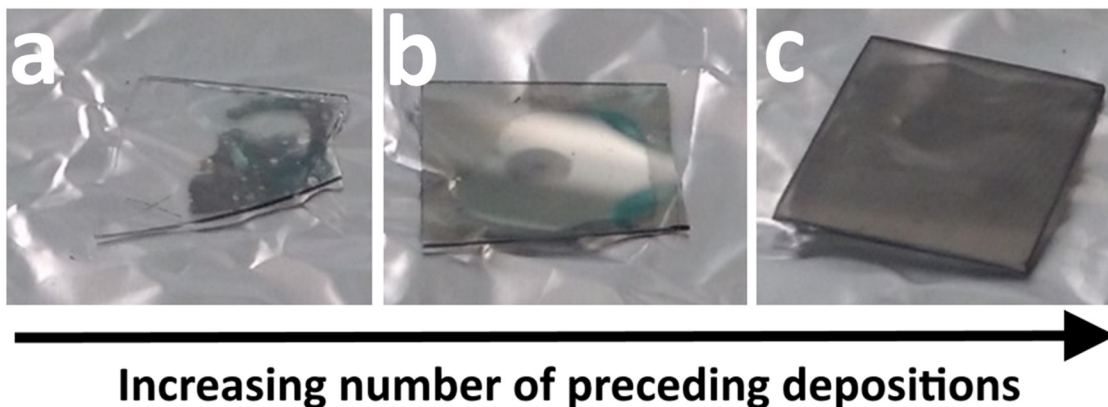


FIG. 22. Sapphire substrates placed on the same spot in the reactor during deposition of cobalt metal by Bis(*N*-*t*-butyl-*N*-ethylpropanimidamido)cobalt(II) and hydrogen. All deposition parameters were the same for the three depositions, the only variable was the number of directly preceding cobalt metal film depositions, with (a) first deposition, (b) second deposition, and (c) fifth deposition. Reproduced with permission from Choudhury *et al.*, presented at the AVS 65th International Symposium & Exhibition (2018). Copyright 2018, D. Choudhury (Ref. 50).

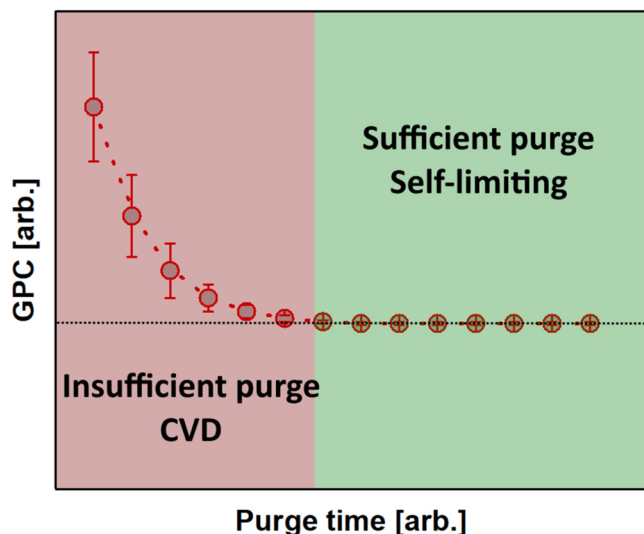


FIG. 23. Typical example of the evolution of growth per cycle as a function of the purge time. Error bars are meant to show that insufficient purge often leads to severe gradients.

longer purge times. The important point is that one needs to optimize the purge time through saturation studies to establish the conditions for self-limiting growth. For a given ALD process, the purge times specified in a paper may not apply to your reactor.

We can further illustrate these purge time effects using the 1D transport model that we presented earlier to examine nonideal surface kinetics and reactor leaks. Figure 24 shows the effect of increasing the diffusivity of one of the two precursors at constant purge time. Increasing the diffusivity is a convenient way to model the effects of insufficient purge in the 1D transport model. Furthermore, Fig. 24 shows that as the diffusivity increases, the GPC increases above the saturation value of 1.0, and the thickness profile becomes less uniform with higher GPC values further upstream. The insufficient purge conditions modeled by the higher diffusivity values lead to precursor mixing and higher GPC values. Depending on both growth conditions and surface kinetics, different growth profiles can be obtained as the magnitude of the CVD component is proportional to the product of the concentration of both species and its evolution over time.

The effects of insufficient purge times are often obvious. However, we reiterate that that linear growth with cycles and a “temperature window” may exist even for non-self-limiting CVD growth. A variable purge time study is the only reliable method to confirm self-limitation during the purge.

As alluded to above, trace impurities in the carrier gas can also cause irreproducibility during ALD that relates to the purge step. However, these problems are much less conspicuous compared to CVD. Even ultrahigh purity nitrogen or argon will contain trace oxygen-containing impurities at the ppm level. These impurities are inconsequential for metal oxide ALD but can dramatically affect the outcome of metal film ALD. Similarly, small leaks in the carrier gas lines are typically not a big issue since these lines are

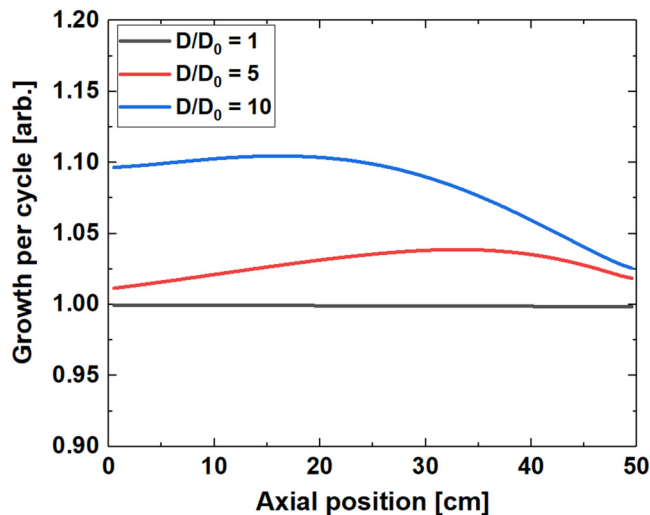


FIG. 24. Impact of cross talk between precursors due to insufficient purging: by increasing the diffusivity D_0 of one of the precursors, the tails of the two doses (e.g., the leading edge of precursor A and the trailing edge of precursor B) overlap in time and space resulting in a CVD component to the growth per cycle. A similar effect is obtained if purge times are shortened.

maintained at an overpressure that prevents the ingress of atmospheric contaminants. However, changing carrier gas cylinders can allow contaminants to diffuse into the lines and eventually show up in the ALD films. Many labs are equipped with nitrogen generators or utilize the boiloff from liquid nitrogen tanks to provide carrier gas. Unfortunately, the age, model, and maintenance level of such a generator, or the procedures followed to change liquid nitrogen tanks, can compromise carrier gas purity. These issues can be extremely difficult to diagnose and rectify.

To illustrate this, Fig. 25 shows what may happen to the growth of three different processes when the purge gas is contaminated with either O_2 or H_2O , shown by mass gain in a theoretical QCM study. $Co(thd)_2$ is a precursor that needs a strong oxidizer such as O_3 to react. The $Co(thd)_2 + O_3 \rightarrow CoO_x$ process would in other words not be affected by water or oxygen contamination at all and would still show self-limitation [Fig. 25(a)]. TMA on the other hand reacts violently with water, and the $TMA + H_2O/O_3 \rightarrow Al_2O_3$ process would be strongly affected by the wet purge gas [Fig. 25(b)]. This would lead to increased (CVD-like) growth during the TMA pulse, lack of self-saturation, and continued reaction during the subsequent purge. Oxygen contamination would have no effect on this process, since TMA does not readily react with oxygen. Finally, the deposition of ruthenium oxide [$Ru(thd)_3 + O_2 \rightarrow RuO_x$] would be strongly affected by oxygen contamination but not by water [Fig. 25(c)].

The effects of impure purge gases are very similar to external leaks, but usually of lower magnitude, and are not so often accompanied by the major gradients that are typical for leaks. The two effects can also be deconvoluted by carrying out a saturation study where the purge gas flow is varied, or shut off completely, while only pulsing one precursor. Increasing growth with increasing inert

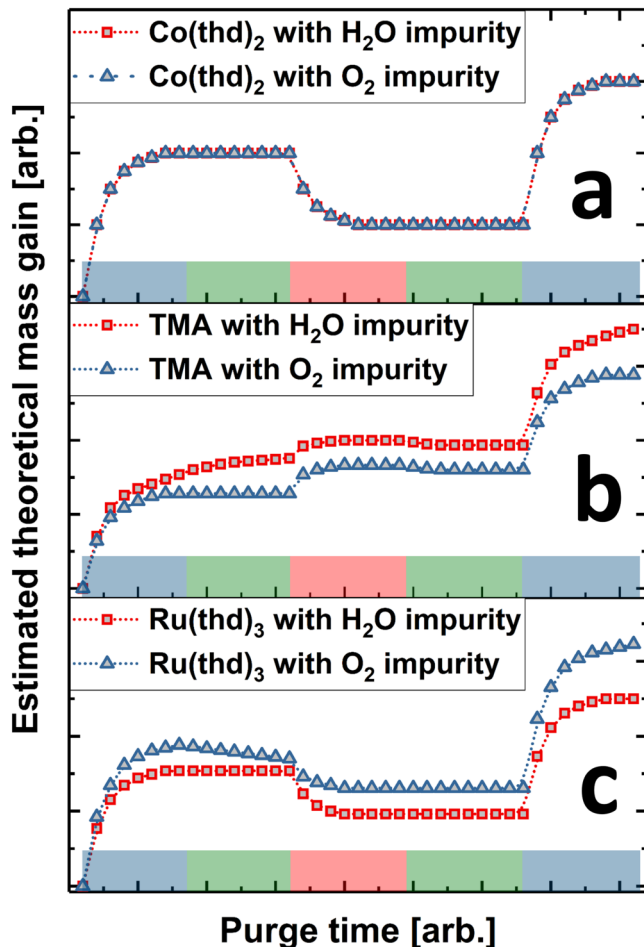


FIG. 25. Estimated theoretical mass gains for (a) $\text{Co}(\text{thd})_2 + \text{O}_3 \rightarrow \text{CoO}_x$, (b) $\text{Al}(\text{CH}_3)_3 + \text{H}_2\text{O} \rightarrow \text{Al}_2\text{O}_3$, and (c) $\text{Ru}(\text{thd})_3 + \text{O}_2 \rightarrow \text{RuO}_x$, when the purging gas has impurities of H_2O (blue triangles) or O_2 (red squares) respectively. Blue, green, and red areas in the x-axis denote cation precursor pulse, purge, and oxidant pulse, respectively.

gas flow during a pulse is an indication that the purge gas is contaminated. Growth without inert gas flow is indicative of an external leak. The fact that impure purge gas will play out very differently on different processes often make it hard to interpret. This is why being confident about the purity level of your inert gas is essential to maintain reproducibility.

IV. SUMMARY AND CONCLUSIONS

Our goal in this paper was to confront the growing acceptance of irreproducibility in ALD by highlighting common sources of error that hamper efforts to duplicate ALD processes developed in a different lab or to reliably perform an ALD process multiple times in one's own lab. While there are numerous issues that affect reproducibility, we have focused on frequently encountered

problems that relate to ALD precursor, substrates, and deposition systems. Our approach was to combine general guidance with examples from the literature and the results of numerical simulations to describe the problem and to illustrate the effects so that the ALD researcher can anticipate and recognize these issues before they cause serious trouble. We feel that this discussion is timely given the rapid expansion in ALD technology driven by the diversity of new applications for ALD films and the broad availability of relatively inexpensive ALD tools. These factors have led to contradictory reports of quantities such as the GPC that should be essentially the same in every lab. The self-limiting surface chemistry that defines ALD should foster reliability and consistency and holds tremendous potential in both research and manufacturing. However, to realize this potential, we should exercise a disciplined approach to determine whether a given process yields self-limiting surface chemistry. Equally important, we should report the conditions in sufficient detail that other researchers, and in particular non-ALD specialists, can reproduce the process in their lab using their equipment.

ACKNOWLEDGMENTS

Henrik H. Sonstebj acknowledges the RIDSEM-project for funding, financed in full by the Research Council of Norway (Project No. 272253). Jeffrey W. Elam was supported as part of the Advanced Materials for Energy-Water Systems (AMEWS) Center, an Energy Frontier Research Center funded by the U.S. Department of Energy, Office of Science, Basic Energy Sciences, under Contract No. DE-AC02-06CH11357.

REFERENCES

- ¹R. L. Puurunen *et al.*, "Overview of doctoral thesis on atomic layer deposition collected in the virtual project on the history of ALD," poster presented at AVS-ALD2019, Bellevue, WA, USA, 21–24 July 2019.
- ²E. Alvaro and A. Yanguas-Gil, *PLoS One* **13**, e0189137 (2018).
- ³V. Miikkulainen, M. Leskelä, M. Ritala, and R. L. Puurunen, *J. Appl. Phys.* **113**, 021301 (2013).
- ⁴B. C. Mallick, C.-T. Hsieh, K.-M. Yin, Y. A. Gandomi, and K.-T. Huang, *ECS J. Solid State Sci. Technol.* **8**, N55 (2019).
- ⁵R. W. Johnson, A. Hultqvist, and S. F. Bent, *Mater. Today* **17**, 236 (2014).
- ⁶H. Salami and A. Poissant, *J. Vac. Sci. Technol. A* **35**, 01B101 (2017).
- ⁷R. Puurunen, *Appl. Surf. Sci.* **245**, 6 (2005).
- ⁸A. W. Ott, K. C. McCarley, J. W. Klaus, J. D. Way, and S. M. George, *Appl. Surf. Sci.* **107**, 128 (1996).
- ⁹R. Kuse, *J. Appl. Phys.* **94**, 6411 (2003).
- ¹⁰A. Tamm *et al.*, *J. Cryst. Growth* **343**, 21 (2012).
- ¹¹A. F. B. Martinson, M. J. DeVries, J. A. Libera, S. T. Christensen, J. T. Hupp, M. J. Pellin, and J. W. Elam, *J. Phys. Chem. C* **115**, 4333 (2011).
- ¹²X. Li, N. C. Fan, and H. J. Fan, *Chem. Vapor Depos.* **19**, 104 (2013).
- ¹³A. V. Plokhikh, M. Falmbigl, I. S. Golovina, A. R. Akbashev, I. A. Karateev, M. Y. Presnyakov, A. L. Vasiliev, and J. E. Spanier, *ChemPhysChem* **18**, 1966 (2017).
- ¹⁴M. Ritala, M. Leskelä, L. Niinistö, and P. Haussalo, *Chem. Mater.* **5**, 1174 (1993).
- ¹⁵H. Döring, K. Hashimoto, and A. Fujishima, *Ber. Bunsen-Ges. Phys. Chem.* **96**, 620 (1992).
- ¹⁶R. Matero, A. Rahtu, M. Ritala, M. Leskelä, and T. Sajavaara, *Thin Solid Films* **368**, 1 (2000).
- ¹⁷M. Reinke, Y. Kuzminykh, and P. Hoffmann, *J. Phys. Chem. C* **120**, 4337 (2016).

- ¹⁸R. Puurunen, *J. Appl. Phys.* **97**, 121301 (2005).
- ¹⁹S. George, *Chem. Rev.* **110**, 111 (2010).
- ²⁰M. Knez, K. Nielsch, and L. Niinistö, *Adv. Mater.* **19**, 3425 (2007).
- ²¹H. H. Sønsteby, H. Fjellvåg, and O. Nilsen, *Adv. Mater. Interfaces* **4**, 1600903 (2017).
- ²²M. D. McDaniel, T. Q. Ngo, S. Hu, A. Posadas, A. Demkov, and J. Ekerdt, *Appl. Phys. Rev.* **2**, 041301 (2015).
- ²³A. Mackus, J. R. Schneider, C. MacIsaac, J. G. Baker, and S. F. Bent, *Chem. Mater.* **31**, 1142 (2019).
- ²⁴M. Ylilammi, *Thin Solid Films* **279**, 124 (1996).
- ²⁵I. Vee, "Hybrid films containing fluorine by ALD," M.Sc. thesis (University of Oslo, 2012).
- ²⁶E. Østreng, O. Nilsen, and H. Fjellvåg, *J. Phys. Chem. C* **116**, 19444 (2012).
- ²⁷S. B. Kim, X. Zhao, L. M. Davis, A. Jayaraman, C. Yang, and R. G. Gordon, *ACS Appl. Mater. Interfaces* **11**, 45892 (2019).
- ²⁸H. H. Sønsteby, E. Østreng, H. Fjellvåg, and O. Nilsen, *Chem. Vapor Depos.* **20**, 269 (2014).
- ²⁹X. Meng, Y. Cao, J. A. Libera, and J. W. Elam, *Chem. Mater.* **29**, 9043 (2017).
- ³⁰A. Devi, *Coord. Chem. Rev.* **257**, 3332 (2013).
- ³¹S. E. Koponen, P. G. Gordon, and S. T. Barry, *Polyhedron* **108**, 59 (2016).
- ³²T. Hatanpää, M. Ritala, and M. Leskelä, *Coord. Chem. Rev.* **257**, 3297 (2013).
- ³³E. Østreng, H. H. Sønsteby, S. Øien, O. Nilsen, and H. Fjellvåg, *Dalton Trans.* **43**, 16666 (2014).
- ³⁴H. H. Sønsteby, K. Weibye, J. E. Bratvold, and O. Nilsen, *Dalton Trans.* **46**, 16139 (2017).
- ³⁵J. Musschoot, Q. Xie, D. Deduytsche, S. Van den Berghe, R. K. Van Meirhaeghe, and C. Detavernier, *Microelectron. Eng.* **86**, 72 (2009).
- ³⁶D. Longrie, D. Deuytsche, J. Haemers, P. F. Smet, K. Driesen, and C. Detavernier, *ACS Appl. Mater. Interfaces* **6**, 7316 (2014).
- ³⁷S. J. Kim, B.-H. Kim, H.-G. Woo, S.-K. Kim, and D.-H. Kim, *Bull. Korean Chem. Soc.* **27**, 219 (2006).
- ³⁸J. W. Elam, M. Schuisky, J. D. Ferguson, and S. M. George, *Thin Solid Films* **436**, 145 (2003).
- ³⁹A. Yanguas-Gil and J. W. Elam, *J. Vac. Sci. Technol. A* **30**, 01A159 (2012).
- ⁴⁰A. Yanguas-Gil, J. A. Libera, and J. W. Elam, *Chem. Mater.* **25**, 4849 (2013).
- ⁴¹H. H. Sønsteby, J. E. Bratvold, K. Weibye, H. Fjellvåg, and O. Nilsen, *Chem. Mater.* **30**, 1095 (2018).
- ⁴²J. W. Elam, A. B. F. Martinson, M. J. Pellin, and J. T. Hupp, *Chem. Mater.* **18**, 3571 (2006).
- ⁴³J. A. Libera, J. N. Hryn, and J. W. Elam, *Chem. Mater.* **23**, 2150 (2011).
- ⁴⁴A. Mackus, M. J. M. Merckx, and W. M. M. Kessels, *Chem. Mater.* **31**, 2 (2019).
- ⁴⁵K. J. Hughes and J. R. Engstrom, *J. Vac. Sci. Technol. A* **30**, 10A102 (2012).
- ⁴⁶P. C. Lemaire, M. King, and G. N. Parsons, *J. Chem. Phys.* **146**, 052811 (2017).
- ⁴⁷J. E. Bratvold, H. H. Sønsteby, O. Nilsen, and H. Fjellvåg, *J. Vac. Sci. Technol. A* **37**, 021502 (2019).
- ⁴⁸V. A.-L. K. Killi, "The role of passivation in the deposition of thin films of K_xNbO_3 ," B.Sc. project thesis (University of Oslo, 2018).
- ⁴⁹H. H. Sønsteby, O. Nilsen, and H. Fjellvåg, *Glob. Chall.* **2019**, 1800114 (2019).
- ⁵⁰D. Choudhury, A. U. Mane, C. M. Patak, A. K. Petford Long, and J. W. Elam, oral presentation at AVS 65th International Symposium & Exhibition, Long Beach, CA, USA, 21–26 October 2018.